

Magnitude distribution of earthquakes: Two fractal contact area distribution

Srutarshi Pradhan^{a,*}, Bikas K. Chakrabarti^{a,†}, Purussatam Ray^{b,‡} and Malay Kanti Dey^c

^a*Condensed Matter Physics Group, Saha Institute of Nuclear Physics,
1/AF, Bidhan Nagar, Kolkata -700 064, India*

^b*Institute of Mathematical Sciences, Chennai, India and*

^c*Variable Energy Cyclotron Center, 1/AF,
Bidhan Nagar, Kolkata -700 064, India*

The ‘plate tectonics’ is an observed fact and most models of earthquake incorporate that through the frictional dynamics (stick-slip) of two surfaces where one surface moves over the other. These models are more or less successful to reproduce the well known Gutenberg-Richter type power law in the (released) energy distribution of earthquakes. During sticking period, the elastic energy gets stored at the contact area of the surfaces and is released when a slip occurs. Therefore, the extent of the contact area between two surfaces plays an important role in the earthquake dynamics and the power law in energy distribution might imply a similar law for the contact area distribution. Since, fractured surfaces are fractals and tectonic plate-earth’s crust interface can be considered to have fractal nature, we study here the contact area distribution between two fractal surfaces. We consider the overlap set (m) of two self-similar fractals, characterised by the same fractal dimensions (d_f), and look for their distribution $P(m)$. We have studied numerically the specific cases of both regular and random Cantor sets (in the embedding dimension $d = 1$), gaskets and percolation fractals (in $d = 2$). We find that in all the cases the distributions show an universal finite size (L) scaling behavior $P'(m') = L^\alpha P(m, L)$; $m' = mL^{-\alpha}$, where $\alpha = 2(d_f - d)$. The $P(m)$, and consequently the scaled distribution $P'(m')$, have got a power law decay with m (with decay exponent equal to d) for both regular and random Cantor sets and also for gaskets. For percolation clusters, $P(m)$ (and hence $P'(m')$) have a Gaussian variation with m .

I. INTRODUCTION

Enormous efforts have been made by geologists and physicists to understand the earthquake phenomena since several decades. Its dynamics is still a challenging problem. Though model studies of earthquake have been going on several decades now, there is no consensus regarding one single model. ‘Plate-tectonics’ is an important observation in this context by the geologists and the Gutenberg-Richter power law is an unique characterisation of this dynamics. The earth’s solid outer crust (about 20 km thick) rests on a tectonic shell. This tectonic shell is divided into a number (about 12) of mobile plates, having relative velocities of the order of few centimeters per year. This motion of the plates arises due to the powerful convective flow of the earth’s mantle, at the

inner core of earth. Due to the surface roughness of both the earth’s crust and the plates, solid-solid frictional forces arise and this helps sticking the earth’s crust to the plates. This sticking develops elastic strains and the strain energy gradually increases because of the uniform motion of the tectonic plates. There is a competition between the sticking frictional force and the restoring elastic force (stress). When the accumulated stress exceeds the frictional force, a slip (earth quake) occurs and it releases the stored additional elastic energy. Gutenberg and Richter (1954) [1], by analysing the records, observed a power-law distribution of the elastic energy released during earthquakes given as $N(\epsilon) \sim \epsilon^{-\alpha}$, where $N(\epsilon)$ is the number of earthquakes releasing energy greater than or equal to ϵ and α is the power exponent. The observed value of α ranges between 0.7 and 1.0. Several hypothesis and model systems have been proposed to investigate the nature of the earthquake phenomena [2]. The main intention of the model studies is to capture the above Gutenberg-

*Electronic address: spradhan@cmp.saha.ernet.in

†Electronic address: bikas@cmp.saha.ernet.in

‡Electronic address: ray@imsc.res.in

Richter type power law for the frequency distribution of failures (quakes) in the failure dynamics of the models. Among these, most of the models [3, 5] incorporate the stick-slip process and the roughness [4] of the surfaces involved as important features. Recently some models [6, 7] have included the fractal nature of both the earth's crust and the plate involved in stick-slip process and initiated new modellings of earthquake dynamics. As the elastic energy can be stored at the contact area of the surfaces only, the contact area distribution should have much importance. Also, in fractal physics the statistics of two fractal overlap is still missing although this may be useful to study the interface properties in many physical situations.

In this report we have studied the contact area distributions and their scaling properties for different sets of fractal surfaces, using computer simulation techniques.

II. SIMULATION STUDIES OF TWO FRACTAL CONTACT AREA DISTRIBUTION

A. Model

Extensive studies have already established different types of fractals and their properties [8, 9, 10]. The statistics of overlaps between two such fractals is however not studied much yet, though their knowledge is often required in various physical contexts. For example, it has been claimed that since the fractured surfaces have got well-characterized self-affine properties, the distribution of the elastic energies released during the slips between two fractal surfaces (earthquake events) may follow the overlap distribution of two self-similar fractal surfaces [6, 7, 14]. Also, using renormalisation group technique Chakrabarti and Stinchcombe [7] have analytically shown that for regular fractal overlap (Cantor sets and carpets) the contact area distribution follows power law.

Here, we study the distribution $P(m)$ of contact area m between two well-characterized fractals having the same fractal dimension. We have chosen different types of fractals: regular or non-random Cantor sets, random Cantor sets (in one dimension), regular and random gaskets on square lattice and percolating clusters [12, 13] embedded in two dimensions. We find a universal scaling behavior of the distribution:

$$P'(m') = L^\alpha P(m, L); m' = mL^{-\alpha}, \quad (1)$$

where L denotes the finite size of the fractal and the exponent $\alpha = 2(d_f - d)$; d_f being the mass dimension of the fractal and d is the embedding dimension. Also the overlap distribution $P(m)$, and hence the scaled distribution $P'(m')$, seen to decay with m or m' following a power law (with exponent value equal to the embedding dimension of the fractals) for both regular and random Cantor sets and gaskets:

$$P(m) \sim m^{-\beta}; \beta = d. \quad (2)$$

For the percolating clusters, however, the overlap distribution takes a Gaussian form. It may

be noted that the normalisation (to unity) restriction on both P and m ensures the same scaling exponent α for both.

B. Overlaps between regular fractals

Here we construct three types of regular fractals: regular Cantor sets of dimension $\ln 2 / \ln 3$, regular Cantor sets of dimension $\ln 4 / \ln 5$ and regular gaskets of dimension $\ln 3 / \ln 2$ on a square lattice. These regular fractals are constructed following a repetitive procedure in successive generations (n) such that the self-similarity is strictly maintained at every stage. For example, a regular Cantor set of dimension $\ln 2 / \ln 3$ is formed in the $n \rightarrow \infty$ limit of the set obtained by removing the middle one-third portion of each occupied set at every generation, starting from a compact set of size $L = 3^n$ at $n = 1$ (see Fig. 1). For the set with dimension $\ln 4 / \ln 5$, one similarly removes the middle one-fifth portion at each generation (here $L = 5^n$ for finite n -th generation).

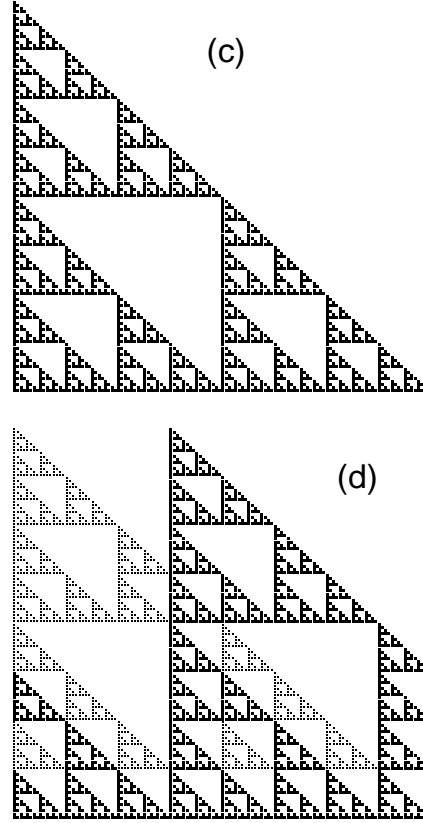
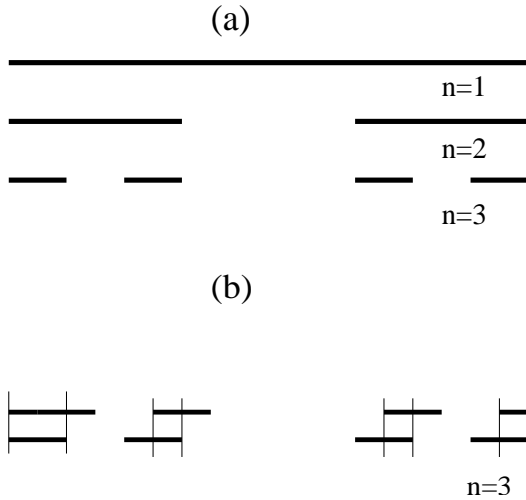


Fig 1: (a) A regular Cantor set of dimension $\ln 2 / \ln 3$; only three finite generations are shown. (b) The overlap of two identical (regular) Cantor sets, at $n = 3$, when one slips over other; the overlap sets are indicated within the vertical lines, where periodic boundary condition has been used. (c) A regular gasket of dimension $\ln 3 / \ln 2$ at the 7th generation. (d) The overlap of two identical regular gaskets at same generations ($n = 7$) is shown as one is translated over the other; periodic boundary condition has been used for the translated gasket.

To study the overlap between two such identical fractals, the boundary effects are avoided using periodic boundary condition for one and we consider the other set to slip over the first. At each step of such slip or translation, we count the overlapping filled sites (black parts or dots) present in both the fractals and the total number of such sites gives the size of overlap m . Thus, if one sequentially translates one fractal over another, various overlap values (m) are obtained which in turn give the distribution $P(m)$. Since no randomness is involved here, we do not need any configurational av-

eraging. These results are shown in Fig. 2, where the Cantor sets and gaskets are generated for finite generations n : $L = 3^n$ for Cantor sets with $d_f = \ln 2 / \ln 3$, $L = 5^n$ for Cantor sets with $d_f = \ln 4 / \ln 5$ and $L = 2^n$ for gaskets with $d_f = \ln 3 / \ln 2$. The overlap distributions $P(m, L)$ are fitted to the scaling forms (1) and (2). The results indicate their validity in the large n (or L) limit.

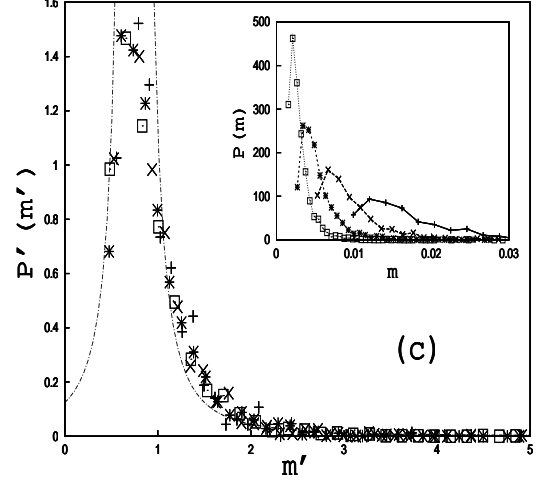
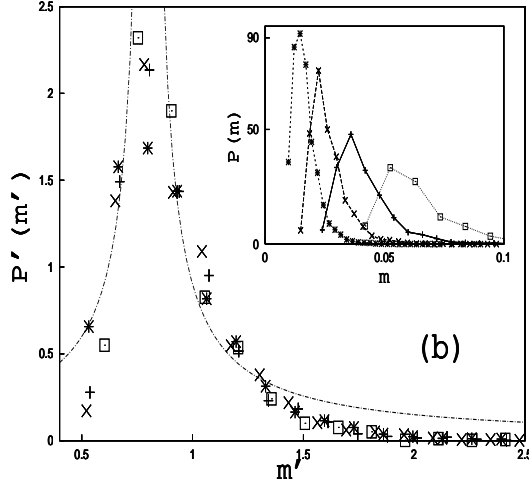
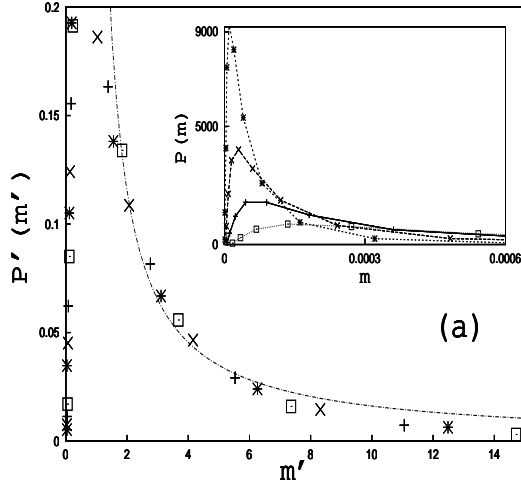


Fig 2: The scaled distribution plot of $P'(m') = P(m, L)L^\alpha$ against the scaled overlap $m' = mL^{-\alpha}$ for two identical regular fractals: (a) Cantor sets with $d_f = \ln 2 / \ln 3$ at various finite generations: $n = 10$ (square), $n = 11$ (plus), $n = 12$ (cross) and $n = 13$ (star); (b) Cantor sets with $d_f = \ln 4 / \ln 5$ for finite generations: $n = 6$ (square), $n = 7$ (plus), $n = 8$ (cross) and $n = 9$ (star); (c) gaskets with $d_f = \ln 3 / \ln 2$ for finite generations: $n = 7$ (plus), $n = 8$ (cross), $n = 9$ (star) and $n = 10$ (square). Note that in all the three cases $\alpha = 2(d_f - d)$ and the dotted lines indicate the best fit curves of the form $a(x-b)^{-d}$; where d is the embedding dimension [$d = 1$ for (a) and (b) and $d = 2$ for (c)]. Insets show the unscaled distributions $P(m)$ for overlap m in different cases.

C. Overlaps between random fractals

Here we construct three types of random fractals: random Cantor sets of dimension $\ln 2 / \ln 3$, random Cantor sets of dimension $\ln 4 / \ln 5$ and random gaskets of dimension $\ln 3 / \ln 2$ on square lattice. We can construct a random Cantor set of dimension $\ln 2 / \ln 3$ by removing randomly any of the one-third portion at every stage or generation (see Fig 3).

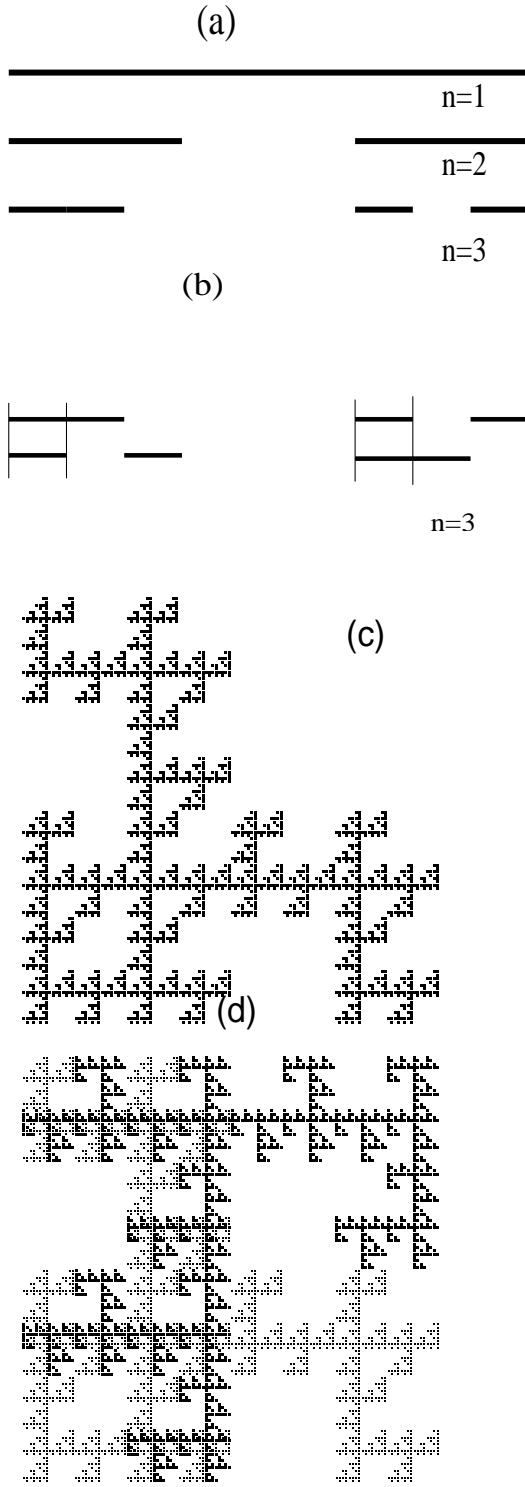
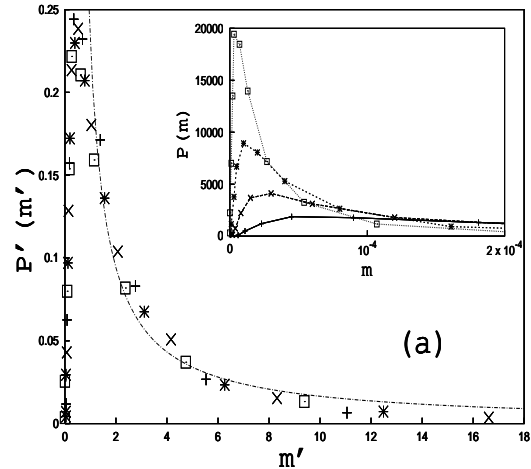


Fig 3: (a) A random Cantor set of dimension $\ln 2 / \ln 3$; only three finite generations are shown. (b) Overlap of two random Cantor sets (at $n = 3$; having the same

fractal dimension) in two different realisations. The overlap sets are indicated within the vertical bars. (c) A random realisation of a gasket of dimension $\ln 3 / \ln 2$ at 7th generation. (d) The overlap of two random gaskets of same dimension and of same generation but generated in different realisations.

Here the structure of the sets change with configurations as randomness is involved. We therefore take the overlap between any two such sets at finite generation n having same dimension but of different configurations. We count the portions present in both the sets, and this gives the total size of overlap m . Clearly the overlap sizes (m) change from one pair of configurations to other and we determine their average distribution $P(m)$. The finite size L of the fractals is similarly related to generation number n as discussed in the previous section. The average distributions $P(m, L)$ for finite size L of the fractals are determined using 500 such configurations for each of the three types of random fractals.



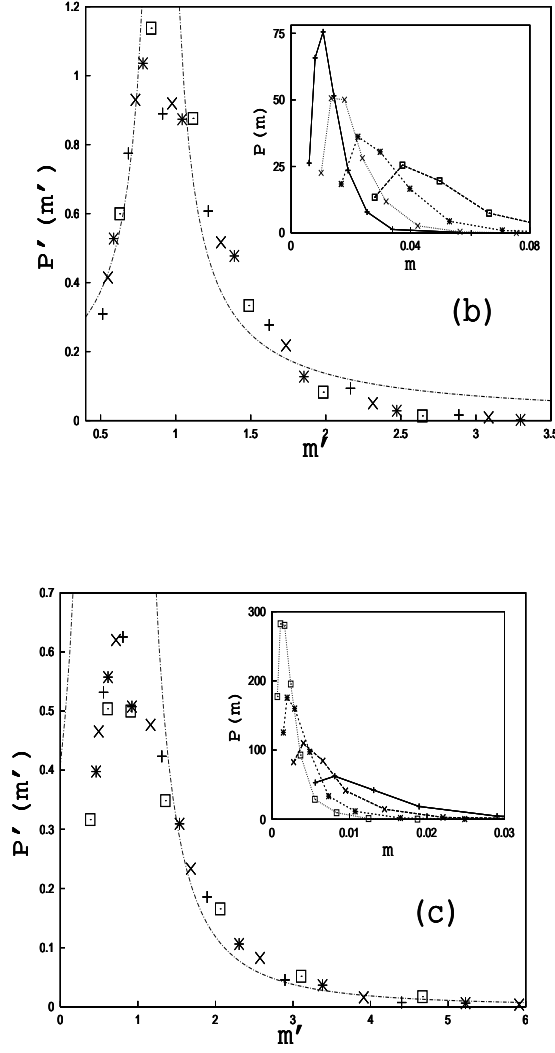


Fig 4: The scaled distribution plot of $P'(m') = P(m, L)L^\alpha$ against the scaled overlap $m' = mL^{-\alpha}$ for random fractals: (a) Cantor sets with dimension $d_f = \ln 2 / \ln 3$ for finite generations: $n = 14$ (square), $n = 13$ (star), $n = 12$ (cross) and $n = 11$ (plus); (b) Cantor sets with $d_f = \ln 4 / \ln 5$ for some finite generations: $n = 10$ (plus), $n = 9$ (cross), $n = 8$ (star) and $n = 7$ (square); (c) gaskets with $d_f = \ln 3 / \ln 2$ for finite generations: $n = 11$ (square), $n = 10$ (star), $n = 9$ (cross) and $n = 8$ (plus). For all the three cases $\alpha = 2(d_f - d)$ and the dotted lines indicate the best fit curves of the form $a(x - b)^{-d}$; where d is the embedding dimension of the fractals [$d = 1$ for (a) and (b) and $d = 2$ for (c)]. Insets show the unscaled distributions $P(m)$ for overlap m .

D. Overlaps of percolating clusters on square lattice

Here we study the overlap distribution of two well-characterised random fractals; namely the percolating fractals [12]. Efficient algorithms are available to generate such fractals. It seems, although many detailed features of the clusters will change with the changes in (parent) fractals, the subtle features of the overlap distribution function remains unchanged.

We generate numerically several site percolating clusters at the percolation threshold ($p_c = 0.5927$ [12]) on square lattices of linear size L using Hoshen-Kopelman algorithm [12, 13]. For the overlap of any two clusters, we count the number of sites M which are occupied in both the clusters (see Fig 5). This gives the overlap size $m = M/L^d$ between the fractals. As the realisations change (keeping the fractal dimension d_f of the percolating cluster same) m varies and we find out its distribution $P(m, L)$. We find that the distribution shifts continuously as L increases and has a finite width which diminishes but very slowly with L . This shows, the emerging length scale associated with m is no longer a constant, rather it depends on L . This arises due to the fractal nature of the original clusters, where the occupation of the sites are no longer random events, but are correlated [12]. Hence, for a system of size L , the probability of occupation grows as L^{d_f} for any of the fractals and as $[L^{d_f}/L^d]^2 = L^{2(d_f-d)}$ for the overlap set. If this is the origin of the L dependence in $P(m, L)$, then the distributions for different L should follow a scaling behavior as indicated by eqn. (1).

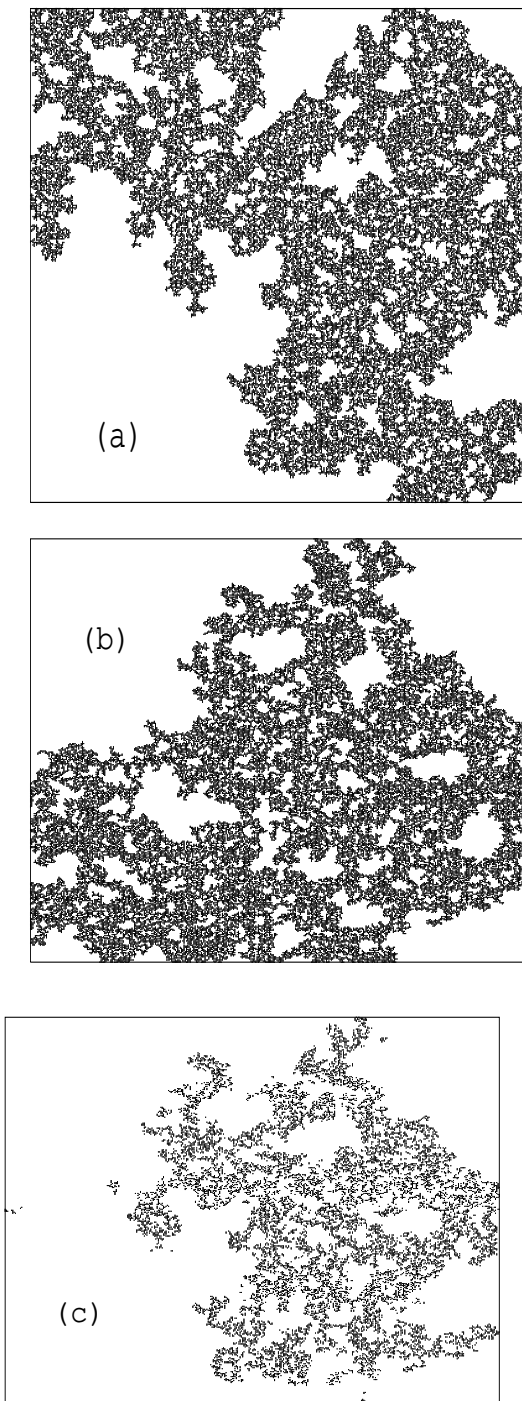


Fig 5: The overlap between two percolating clusters; (a) and (b) are two typical realisations of the same percolating fractal on square lattice ($d_f \simeq 1.89$) and (c) their overlap set. Note, the overlap set need not be

a connected one.

From the overlap between all the pairs of cluster configurations (typically around 500 for $L = 400$), we determine the distribution $P(m, L)$. The data are binned to facilitate storage and to make the distribution smooth (Fig 6 (a)). We have also studied the nature of the distribution $P(m)$ for percolation clusters generated with lattice occupation probability p above p_c of the square lattice. Here the distributions become delta functions and the height of the delta function increases with system size L (Fig 6 (b)).

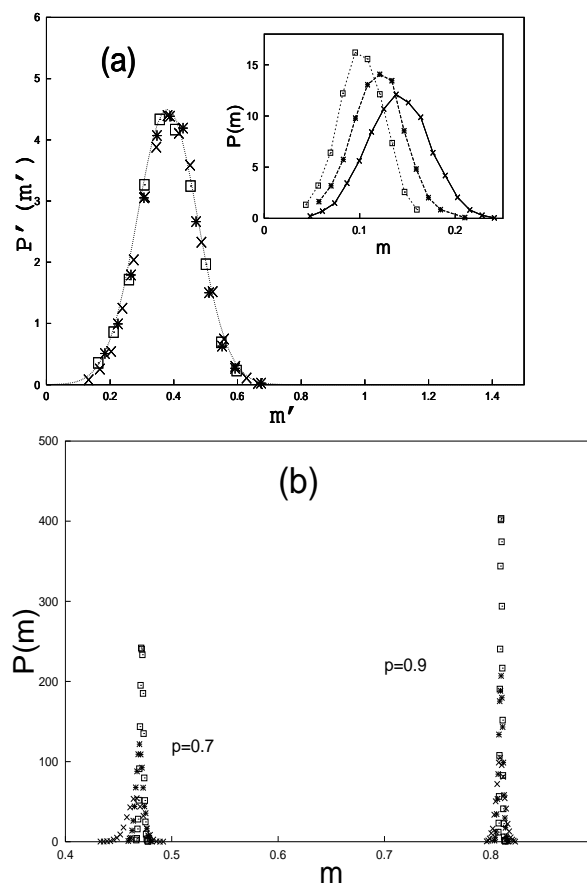


Fig 6: (a) The scaled distribution plot of $P'(m') = P(m, L)L^\alpha$ against the scaled overlap $m' = mL^{-\alpha}$ for percolating clusters grown with probability $p = p_c = 0.5927$ on square lattice ($d_f \simeq 1.89$) for finite sizes: $L = 100$ (cross), 200 (star) and 400 (square). Here $\alpha = 2(d_f - d)$. The dotted line indicates the best fit curve of the form $a \exp(-(x - b)^{2.0}/c)$; where $a (= 4.5)$, $b (= 0.38)$ and $c (= 0.018)$ are constants. Inset shows the unscaled distribution $P(m)$ against overlap

size m . (b) The distribution $P(m)$ against overlap size m for percolation clusters generated with occupation probability p above p_c ($p = 0.7$ and $p = 0.9$) on square lattice [for finite sizes: $L = 100$ (cross), 200 (star) and 400 (square)]. Clearly the distributions $P(m)$ are delta functions and the height of the delta function increases with the system size L .

III. CONCLUSION

In the context of studying the earthquake magnitude distribution, we have studied here a model where the earthquake fault and the moving tectonic plates are assumed to be self-similar fractals. Essentially, we study the contact area distribution of two nominally identical fractals. Our study on different sets of fractal surface overlap shows that the contact area distributions are not always power laws. Although for Cantor sets and gaskets having different fractal dimensions (both for regular and random cases), the contact area distributions have got power laws, for percolating clusters (at percolation threshold) it takes

a robust Gaussian form which we can't explain even qualitatively. In particular, we find that in all the cases the distributions $P(m, L)$ show an universal finite size (L) scaling behavior $P'(m') = L^\alpha P(m, L)$; $m' = mL^{-\alpha}$, where $\alpha = 2(d_f - d)$. The $P(m)$, and consequently the scaled distribution $P'(m')$, have got a power law (2) decay with m (with decay exponent equal to d) for both regular and random Cantor sets and also for gaskets. For percolation clusters, $P(m)$ (and hence $P'(m')$) have a Gaussian variation with m (Fig. 6a). It may be mentioned that, since in many cases the bulk thermodynamics may be mapped to some reduced dimensional interface problems and since their overlaps corresponds to physical quantities (e.g., the replica overlap in the physics of glasses [11]), such fractal overlap distributions are of quite general interest.

Acknowledgement: We are grateful to Prof. D. Stauffer for his useful comments and for a critical reading of the manuscript. We are also thankful to A. Hansen and J. Kertesz for their comments.

-
- [1] Gutenberg, B. and Richter, C. F. (1954). *Seismicity of the Earth and Associated phenomena*, Princeton University Press, Princeton, N.J.
 - [2] See e.g., B. K. Chakrabarti, L. G. Benguigui, *Statistical Physics of Fracture and Breakdown in Disorder Systems*, Oxford Univ. Press, Oxford, 1997.
 - [3] R. Burridge, L. Knopoff, *Bull. Seis. Soc. Am.* 57 (1967) 341-371.
 - [4] A. Hansen and J. Schmittbuhl, *Phys. Rev. Lett.* 90, 045504 (2003); J. Schmittbuhl, A. Hansen and G. G. Batrouni, *Phys. Rev. Lett.* 90, 045505 (2003).
 - [5] J. M. Carlson, J. S. Langer, *Phys. Rev. Lett.* 62 (1989) 2632-2635.
 - [6] V. De Rubeis et al, *Phys. Lett.* 76 (1996) 2599-2602.
 - [7] Chakrabarti, B. K., Stinchcombe, R. B. *Physica A*, 270 (1999) 27-34.
 - [8] Barabasi, A. L. and Stanley, H. E. (1995), *Fractal Concepts in Surface Growth*, Cambridge University Press, Cambridge.
 - [9] P. Bak, *How Nature Works*, Oxford Univ. Press, Oxford (1997)
 - [10] B. B. Mandelbrot, *The Fractal Geometry of Nature* (Freeman, San Francisco, 1982).
 - [11] See e.g., A. P. Young, (Ed), *Spin Glasses and Random Fields* (World Scientific, Singapore, 1999).
 - [12] See e.g., D. Stauffer and A. Aharony, *Introduction to Percolation Theory* (Taylor and Francis, London, 1994).
 - [13] P. L. Leath, *Phys. Rev.* **B14**, 5046 (1976); Z. Alexandrowitz, *Phys. Lett.* **80A**, 284 (1980).
 - [14] B. K. Chakrabarti, M. K. Dey, S. Pradhan, *Fracture Dynamics and Earthquake Models*, unpublished (2000).